HORIZONTAL AXIS WIND TURBINE POST STALL AIRFOIL CHARACTERISTICS SYNTHESIZATION

James L. Tangler
Rockwell International
Wind Energy Research Center
Golden, Colorado 80402-0464

Cyrus Ostowari
Texas A&M University
College Station, Texas 77843-3141

ABSTRACT

Blade-element/momentum performance prediction codes are routinely used for wind turbine design and analysis. A weakness of these codes is their inability to consistently predict peak power upon which the machine structural design and cost are strongly dependent. The purpose of this study was to compare post-stall airfoil characteristics synthesization theory to a systematically acquired wind tunnel data set in which the effects of aspect ratio, airfoil thickness, and Reynolds number were investigated. The results of this comparison identified discrepancies between current theory and the wind tunnel data which could not be resolved. Other factors not previously investigated may account for these discrepancies and have a significant effect on peak power prediction.

1. INTRODUCTION

The cost of a wind turbine is influenced by the designer's ability to predict peak power. Uncertainty in the performance prediction codes for predicting peak power forces the designer to be conservative and oversize the generator and other mechanical components. This practice leads to higher machine cost which in turn increases the resulting energy cost. The ability to predict peak power is dependent on an accurate description of the airfoil lift and drag characteristics immediately after stall. As a rotor approaches peak power, aerodynamic stall progressively envelopes the blade from root to tip. At peak power the root end of the blade is deeply stalled and the tip region, where most of the power is being developed, is passing through the angle of attack range of 15 to 25 degrees. Peak power is most sensitive to the airfoil characteristics over this angle of attack range.

Blade-element/momentum performance prediction codes provide the principle means for rotor design and analysis. With the use of reasonable airfoil data, these codes have been able to provide good estimates of rotor performance provided a substantial portion of the blade is not stalled. Past experience has shown that, for a fixed pitch rotor, when a large portion of the blade is stalled the use of two-dimensional (2-D) airfoil data under-predicts peak power and shows a rapid drop off thereafter relative to measured power. A detailed discussion of this problem is contained in References 1 and 2. The under-prediction of peak power has motivated the development of 3-D post stall airfoil data synthesization routines (References 3 and 4). Of these two routines, that of Reference 3 is more widely used because of its user friendly nature. Without any user interaction the routine automatically provides a smooth curve fit from where the 2-D airfoil data leaves off up through the highest angle of attack experienced by the blade during stall. The approach of Reference 4 is more subjective and requires the user to provide discrete airfoil data in the light stall region. Both of these routines are based on past studies which show that after stall the airfoil characteristics of lift and drag are strongly governed by blade aspect ratio and are relatively independent of the airfoil geometry and Reynolds number. After stall, lower aspect ratios result in lower values of lift and drag coefficients due to greater flow leakage around the tip that relieves the pressure differential across the blade.

Although the 3-D post-stall airfoil data synthesization routines provided the needed direction to help solve the peak and post-stall power prediction problem an adequate post-stall airfoil data base was not available at the time of their development. Consequently, these methods were tailored to predict peak power based on comparisons for a few machines. Applied to other machines these methods were suspect when predicted and measured peak power were not in agreement. For this reason, it was widely held that the 3-D post-stall synthesization routines needed further verification against a comprehensive post-stall airfoil data base. In an effort to satisfy this need, post-stall airfoil data were acquired in the Texas A&M University wind tunnel.

2. POST STALL WIND TUNNEL TEST

To establish the data base to better verify the post stall synthesization theory, nonrotating wing sections were tested in the Texas A&M 7 x 10 ft wind tunnel. Post stall performance characteristics were established as a function of aspect ratio, airfoil thickness, and Reynolds number. For this purpose the test models had a one foot chord and were of the NACA 44XX family of airfoils. Blade aspect ratios of 6, 9, and 12 and ∞ were tested for airfoil thicknesses of 9, 12, 15, and 18 percent at Reynolds numbers of 250,000, 500,000, 750,000 and 1,000,000. The results from this study showed that the post stall airfoil characteristics of C_L and C_D are a strong function of aspect ratio as expected and a weak function of airfoil thickness. In the post stall region the influence of Reynolds number was negligible for the range tested. A report (Reference 5) containing the results from this study and can be obtained from Rocky Flats Wind Energy Research Center (WERC).

Two plots extracted from this report which illustrate the influence of aspect ratio on C_L and C_D are shown in Figures 1 and 2. Figure 1 shows C_D versus angle of attack for the four aspect ratios. For discussion purposes the figure can be broken down into three distinct angle of attack regions. In the

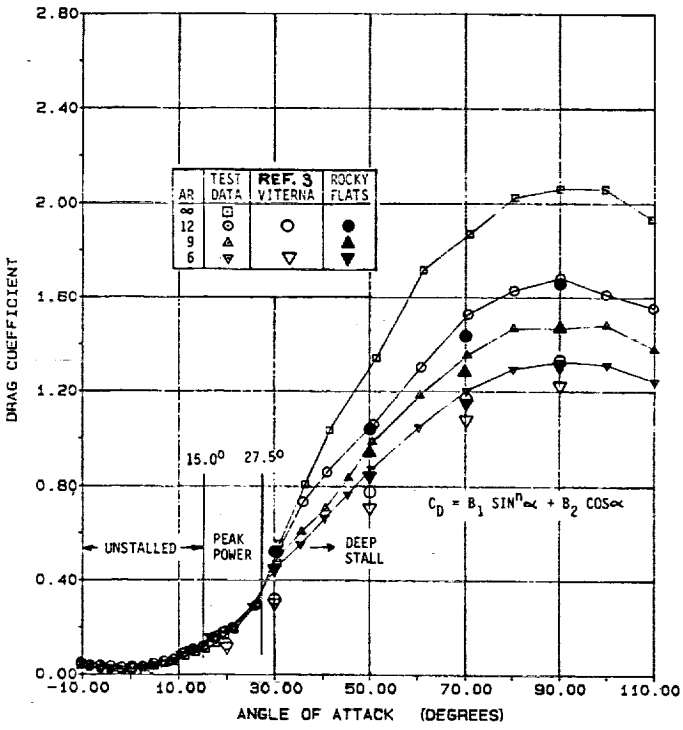

Fig. 1. Effect of Aspect Ratio on Drag Coefficients of the NACA 4418 Airfoil at RN = 0.25 x 10^6.

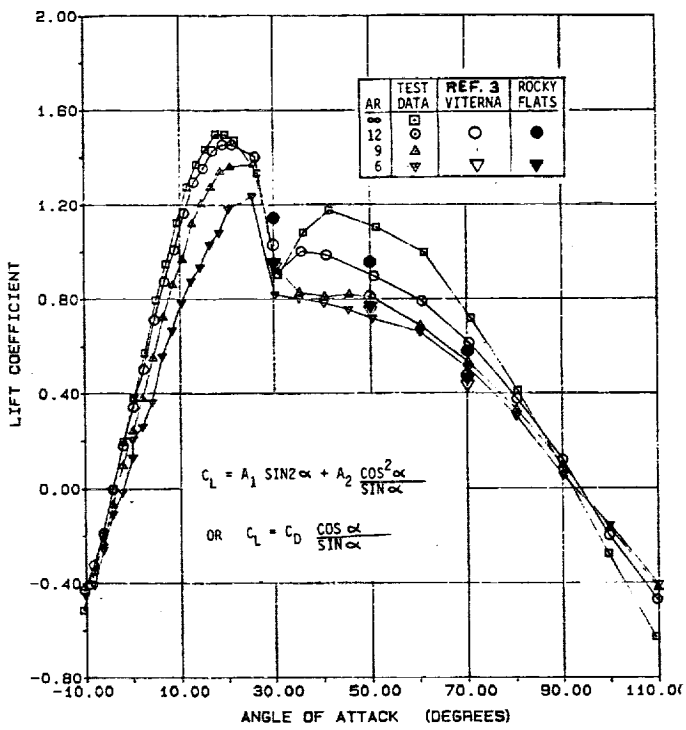

Fig. 2. Effect of Aspect Ratio on Lift Coefficients of the NACA 4418 Airfoil at RN = 0.25 x 10^6.

TABLE 1. POST STALL C_L, C_D EQUATIONS

Equations of Reference 3

$$C_{D_{max}} = 1.11 + 0.018\ AR \qquad @\ (\alpha=90°) \qquad (1)$$

$$C_D = B_1 \sin^2\alpha + B_2 \cos\alpha \qquad (\alpha=15°\text{to}90°) \qquad (3)$$

where:

$$B_1 = C_{D_{max}}$$

$$B_2 = \frac{C_{D_s} - C_{D_{max}} \sin^2\alpha_s}{\cos\alpha_s}$$

$$C_L = A_1 \sin 2\alpha + A_2 \frac{\cos^2\alpha}{\sin\alpha} \qquad (\alpha=15°\text{to}90°) \qquad (5)$$

where:

$$A_1 = B_1/2$$

$$A_2 = (C_{L_s} - C_{D_{max}} \sin\alpha_s \cos\alpha_s)\frac{\sin\alpha_s}{\cos^2\alpha_s}$$

Equations Derived from Texas A&M Data

$$C_{D_{max}} = \frac{1.00 + 0.065\ AR}{(0.9 + t/c)} \qquad @\ (\alpha=90°) \qquad (2)$$

$$C_D = B_1 \sin\alpha + B_2 \cos\alpha \qquad (\alpha=27.5°\text{to}90°) \qquad (4)$$

where:

$$B_1 = C_{D_{max}}$$

$$B_2 = \frac{C_{D_s} - C_{D_{max}} \sin\alpha_s}{\cos\alpha_s}$$

α	C_D
16°	0.100
20°	0.175
25°	0.275
27.5°	0.363

Same as equation 5, however the use of the new $C_{D_{max}}$ for evaluating A_1 and A_2 results in a stronger AR influence.

alternate: $C_L = C_D \frac{\cos\alpha}{\sin\alpha}$ $\qquad (\alpha=30°\text{to}90°) \qquad (6)$

with: $C_L = 0.9$ $\qquad @\ \alpha=30°$

AR - aspect ratio
C_D - drag coefficient
C_L - lift coefficient
t/c - non-dimensional airfoil thickness
α - angle of attack
α_s - angle of attack at stall, usually 15°

first region up to 15 degrees, the wings are unstalled and for performance prediction purposes similar 2-D airfoil data for this region is normally acquired from one of many airfoil data catalogs for a desired Reynolds number. However, for this 3-D testing induced drag effects steadily increase with angle of attack with the magnitude being greater for lower aspect ratios. This subtle trend is masked by the accuracy of the data over this angle of attack range. The second angle of attack region from 15 to 27.5 degrees is worthy of special attention since it has the dominant effect on peak power prediction. An important characteristic of this region is that aspect ratio effects cannot be discerned. In this region the higher induced drag associated with lower aspect ratio is neutralized by the lower pressure drag associated with lower aspect ratio. Aspect ratio effects are not seen to have a net influence on drag coefficient until the angle of attack exceeds 27.5 degrees. Above this angle the pressure force across the wing increases as the tip relief diminishes with aspect ratio.

For comparative purposes the post stall synthesization equations of Reference 3 were used to generate corresponding values of C_L and C_D. The calculated values are compared to the test data over the angle of attack range of 20 to 90 degrees as shown by the large open symbols for aspect ratios of 6 and 12. For both aspect ratios the calculated values fall well below measured values. In addition, the equations lack the strong sensitivity to aspect ratio as shown by the data above a 30 degree angle of attack. To better reflect the measured first order aspect ratio and second order airfoil thickness effects, equations 2 and 4 are presented for $C_{D_{max}}$ and C_D, respectively. These equations were used to generate the shaded symbols and show good agreement with test results over the angle of attack range of 27.5 to 90 degrees. The new maximum drag coefficient equation has three times greater sensitivity to aspect ratio. In addition further aspect ratio sensitivity was acquired by using a first order (Sin) term in the drag coefficient equation. The new approximation (Equation 4) only applies over the angle of attack range of 27.5 to 90 degrees versus 15 to 90 degrees used in the original approximation (Equation 3). The discrete values of drag shown in Table 1 for the angle of attack range of 16 to 27.5 degrees are for airfoils having thickness of 12 percent or greater. The wind tunnel test results show that for thinner airfoils a more rapid increase in drag can be anticipated over this local angle of attack range. A step jump in drag is needed to transition from 2-D data to discrete 3-D data. An increase to a value of 0.10 appears reasonable in going from 15 to 16 degrees.

A comparison of the calculated measured lift coefficient versus angle of attack is shown in Figure 2 for the various aspect ratios. Prior to stall a reduction in aspect ratio reduces the slope of the C_L curve. In blade-element/momentum type analyses this trend is approximated through the use of the tip loss factor. In the post stall region the measured lift coefficient undergoes a rapid initial drop off followed by a moderate reduction in C_L up until the angle of attack region of 60 degrees. An approximation of this post stall behavior is obtained using Equation 5 from Reference 3. The equation provides a continuous drop off from peak C_L to zero at 90 degrees in a manner characteristic of the test data. The equation makes no attempt to approximate the initial drop and recovery the C_L experiences for the higher aspect ratio blades. However, this simplification does not appear to result in significant error. Calculated values of C_L are shown by the large open symbols using this equation with the values of A_1 and A_2 based on the old $C_{D_{max}}$ (Equation 1) as given in Reference 3. Calculated values of C_L using the new $C_{D_{max}}$ (Equation 2) to determine A_1 and A_2 are shown by the solid symbols. Stronger aspect ratio dependency and somewhat better agreement is achieved using the new approximation for $C_{D_{max}}$. This equation provides good results from peak C_L throughout most of the post stall region which typically begins around 15 degrees for most airfoils.

Two interesting characteristics of these data in Figures 1 and 2 is that although the magnitude of C_L and C_D are a function of aspect ratio, the ratio of C_L/C_D for a given angle of attack is found to be independent of aspect ratio throughout the deep stall angle of attack range over 30 degrees. In addition, C_L/C_D or more appropriately L/D, passes exactly through a value of 1.0 at an angle of attack of 45 degrees as would a flat plate. These characteristics are shown by the square symbols in Figure 3. For comparison flat plate theory is represented by the solid line as calculated by the equation $L/D = \cos\alpha/\sin\alpha$. The data points of L/D are seen to approximate the ratio of $\cos\alpha/\sin\alpha$ over the angle of attack range of 30 through 60 degrees. Beyond this point the data points fall above flat plate theory due to the suction developed by the leading edge curvature. Based on this trend equation 5 can be replaced by the flat plate theory alternate of equation 6. Using equation 5, the ratio of L/D will be somewhat on the high side throughout the angle of attack range and will not quite satisfy the observation that L/D = 1 at an angle of attack of 45 degrees as does equation 6.

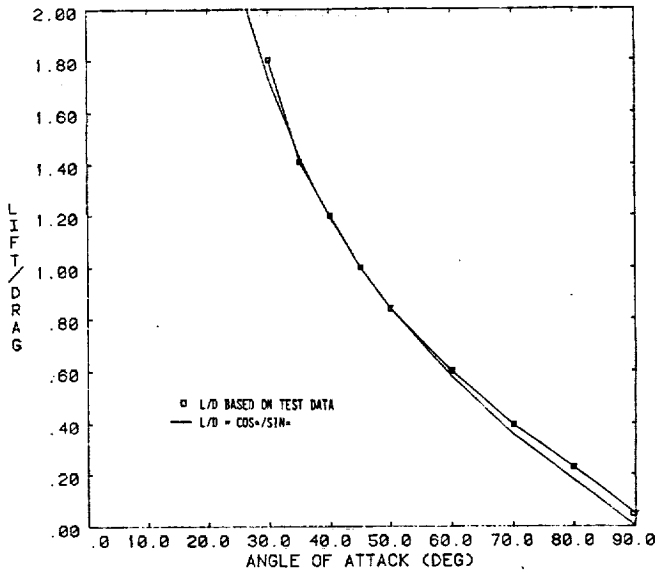

Fig. 3 Effect of Aspect Ratio on Lift/Drag Ratio in Deep Stall

3. PEAK POWER PREDICTIONS

Predicted performance was calculated for three fixed pitch wind turbines using Rocky Flats blade-element/ momentum analysis (PROPSH) which is described in Reference 2. Using both the post stall airfoil data synthesization method of Reference 3 and the modified equations based on the Texas A&M wind tunnel data predicted peak power was compared to measured peak power. The machines analyzed were the Jay Carter 25, ESI-54, and the MOD-0. In each case predicted peak power was calculated on the low side of measurements by 3 to 15 percent using the modified equations based on the Texas A&M wind tunnel data. Better agreement was achieved using the synthesization method of Reference 3. Calculated peak power relative to measured power varied from being 2 percent on the low side to 8 percent on the high side. Overall the modified equations based on the wind tunnel data predicted peak power 3 to 12 percent lower than the equations of Reference 3 which were developed by tailoring the equations to correlate with actual peak power measurements.

The better agreement achieved using the equations of Reference 3 is attributed mainly to the higher L/D resulting in the angle of attack range of 15 to 30 degrees. As previously indicated this portion of the post stall region has the greatest impact on peak power prediction. Another factor not to be overlooked is the accuracy of $C_{L_{max}}$ associated with the 2-D data tables used in the calculations. Any error in the $C_{L_{max}}$ utilized translates into a similar error in the value of peak power.

Speculation as to the difference in L/D resulting from the lift and drag equations of Reference 3 versus the lower L/D resulting from the modified equations based on the Texas A&M wind tunnel data yields some potential explanations. The Texas A&M wind tunnel tests were nonrotational. Aerodynamicists over the years have speculated that for rotating wings centrifugal force effects are present in the boundary layer that result in spanwise flow toward the blade tip. Spanwise flow is thought to enhance performance by delaying separation of the boundary layer. Another source of spanwise flow is the spanwise suction gradient that results from the rotating blades local oncoming velocity being proportional to the blade radius. For both of the these causes, the spanwise flow is from blade root to blade tip.

A second scenario that warrants serious consideration when trying to account for low peak power predictions deals with elastic twist of the blade. Prior to stall many airfoils have little or no nose down (negative) pitching moment. When stall occurs in the angle of attack range of 15 to 30 degrees, the moment coefficient rapidly diverges. The resulting large increase in nose down pitching moment can result in elastic twist toward feather which would enhance the power output and delay stall. The twist effect would become greater with windspeed as the stall enveloped the blade while propagated outward toward the tip. The occurrence of just a couple of degrees of elastic twist with increasing windspeed would substantially enhance peak power and post peak power. Elastic twist is a real consideration the manufacturer should be aware of because of its strong influence on measured post stall power. The degree of elastic twist can be expected to vary from one machine to another depending on the amount of blade torsional stiffness.

4. CONCLUDING REMARKS

The Texas A&M post stall wind tunnel test of the NACA 44XX series airfoils as influenced by airfoil thickness, Reynolds number, and aspect ratio yielded the following findings.

- Reynolds number was found to have an insignificant influence on the airfoil characteristics over the range of 250,000 to 1,000,000.
- Airfoil thickness was found to have little effect on post stall C_L although it does influence $C_{L_{max}}$ which is normally acquired from a 2-D airfoil data catalog. Increased thickness did provide some reduction in drag throughout the post stall region.
- Aspect ratio was the dominant influence on the post stall airfoil characteristics. However, this influence was not readily discerned over the angle of attack range of 15 to 30 degrees where the lower induced drag associated with high aspect ratios is being neutralized by a corresponding increase in pressure drag. Above 30 degrees both drag coefficient and lift coefficient increased with aspect ratio such that the resulting ratio of L/D was independent of aspect ratio.

Applying these test results the post stall synthesization equations of Reference 3 were modified. Peak power predictions using the newly modified equations and those of Reference 3 showed that:

- the modified equations underpredicted peak power by 3 to 15 percent
- the equations of Reference 3, because of their more optimistic post stall L/D ratio, provided a better approximation of peak power.

Potential causes of the differences between measured peak power and that predicted using the modified equations based on the Texas A&M data are:

- the inability of nonrotating wind tunnel test to represent the influence of radial flow effects
- elastic twists effects resulting from the divergence of the post stall moment coefficient.

REFERENCES

1. "First Meeting of Specialists on the Aerodynamics of Horizontal-Axis Wind Turbines," Sponsored by Rocky Flats Wind Energy Research Center and NASA Wind Energy Project Office, Wichita, Kansas, April 20-21, 1983.
2. Tangler, J. L., "Assessment of Blade-Element/ Momentum Analysis for Horizontal-Axis Wind Turbines," Sixth Biennial Wind Workshop, Minneapolis, Minnesota, June 1983.

3. Viterna, L. A. and Corrigan, R. D., "Fixed Pitch Rotor Performance of Large Horizontal Axis Wind Turbines," paper presented at the DOE/NASA Workshop on Large Horizontal Axis Wind Turbines, (Cleveland, Ohio), July 28-30, 1981.

4. Hibbs, B, and Radkey, R. L., "Calculating Rotor Performance with the Revised 'PROP' Computer Code," RFP-3508 UC-60, February 1983.

5. Ostowari, C., and Naik, D., "Post Stall Wind Turbine Studies of Varying Aspect Ratio Wind Tunnel Blades with NACA 44XX Series Airfoil Sections," RFP-_____, June 1984.

NOTICE

The work reported in this paper was performed under contract No. DE-AC04-76DP03533 for the U.S. Department of Energy.